Luminescence properties of Sm^{3+}-doped P_2O_5–PbO–Nb_2O_5 glass under high pressure

2009 J. Phys.: Condens. Matter 21 035108

(http://iopscience.iop.org/0953-8984/21/3/035108)

IOP Publishing Journal of Physics: Condensed Matter

J. Phys.: Condens. Matter **21** (2009) 035108 (9pp) doi:10.1088/0953-8984/21/3/035108

Luminescence properties of Sm^{3+}-doped P_2O_5–PbO–Nb_2O_5 glass under high pressure

R Praveena[1], V Venkatramu[2], P Babu[3], C K Jayasankar[1,6], Th Tröster[4], W Sievers[5] and G Wortmann[5]

[1] Department of Physics, Sri Venkateswara University, Tirupati-517 502, India
[2] Department of Physics, Yogi Vemana University, Kadapa-516 003, India
[3] Department of Physics, Government Degree and P.G. College, Wanaparthy-509 103, India
[4] Fakultät für Maschinenbau, Universität Paderborn, Paderborn D-33098, Germany
[5] Department Physik, Universität Paderborn, Paderborn D-33095, Germany

E-mail: ckjaya@yahoo.com

Received 13 August 2008, in final form 4 November 2008
Published 10 December 2008
Online at stacks.iop.org/JPhysCM/21/035108

Abstract

Samarium doped lead phosphate glass modified with niobium having a composition (in mol%) of $55P_2O_5 + 39.5PbO + 5Nb_2O_5 + 0.5Sm_2O_3$ has been prepared by the conventional melt quenching technique. The emission spectra and the decay curves for the $^4G_{5/2}$ level of Sm^{3+} ions have been measured as a function of pressure up to 23.6 GPa at room temperature. A discontinuity in the observed shifts and crystal-field splittings as a function of pressure around 9–10 GPa suggests that a phase transition is taking place in the glass matrix. The $^4G_{5/2} \rightarrow {}^6H_{5/2}$, $^6H_{7/2}$ and $^6H_{9/2}$ transitions are shifted towards the lower energy side with magnitudes of −7.1, −7.6 and −5.5 cm^{-1} GPa^{-1} up to 8.9 GPa (phase 1) and −5.6, −4.9 and −4.4 cm^{-1} GPa^{-1} beyond 10.3 GPa (phase 2), respectively. A much stronger increase in the splitting of the $^4G_{5/2} \rightarrow {}^6H_{5/2}$ and $^4G_{5/2} \rightarrow {}^6H_{7/2}$ Stark levels with pressure is observed in phase 1 than in phase 2. The lifetime of the $^4G_{5/2}$ level decreases from 2.29 ms (0 GPa) to 0.64 ms (23.6 GPa) with pressure. The decay curves of the $^4G_{5/2}$ level exhibit non-exponential behavior for all the pressures and were fitted by the generalized Yokota–Tanimoto model to probe the nature of the energy transfer process. The best fits with $S = 6$ indicate that the energy transfer between donor and acceptor is of dipole–dipole type. The crystal-field splitting experienced by the Sm^{3+} ions in the title glass are found to be larger than those found in borate, K–Ba–Al phosphate and tellurite glasses.

1. Introduction

Rare earth (RE) ions play an important role in modern optical technology as the active constituents in many novel materials. There is an increasing number of applications for these RE-activated materials and much of today's cutting-edge optical technology and future innovations are expected to rely on their unique properties [1–4]. In particular, the use of RE ions emitting in the optical fiber spectral region has attracted considerable interest as a new field of luminescent materials [5, 6]. Luminescence properties of RE ions are intimately connected with their 4f-electron configuration and controlled by tuning the chemical and physical interactions in the nearest neighbor coordination shell, where factors such as bond lengths, bond angles, coordination number and covalency determine the energy and crystal-field (CF) splitting of the 4f multiplets involved in luminescence [7]. Physical interaction due to application of high pressure has the ability to tune continuously the interatomic distances and bond angles between RE ions and ligands. Hence, optical properties of RE doped materials can be continuously varied without changing the chemical composition. Pressure-induced variations of optical properties include lifetimes, cross-sections, linewidths,

[6] Author to whom any correspondence should be addressed.

peak positions, etc, which can give valuable information concerning the interaction of the RE ion with its surroundings.

Glasses containing Sm^{3+} ions have stimulated extensive interest due to their potential application for high-density optical memory devices [8, 9]. The emitting $^4G_{5/2}$ level of Sm^{3+} ions in the visible region exhibits relatively high quantum efficiency and shows different quenching emission channels, which make Sm^{3+} ions an interesting case to analyze the energy transfer process [10–13]. Recently, phosphate glasses have received a great deal of attention due to their considerable applications in optical data transmission, detection, sensing and laser technologies [14]. Phosphate glasses have unique characteristics that include high transparency, low melting point, high thermal stability, high gain density due to a high solubility for RE^{3+} ions, low refractive index and low dispersion [15].

Niobium phosphate glasses have attracted extensive investigations in recent years because of their wide range of applications such as waste immobilization of radioactive materials [16–21]. These glasses are also found to have exceptionally high optical quality and high gain, with minimum beam divergence when used as laser hosts [22]. Further, there has been an increasing academic and technological interest in the structural role of the Nb^{5+} ions and their interaction with the other ions in the glass network [23–26]. Investigations of different niobium phosphate glasses mixed with a variety of modifier oxides like BaO, K_2O etc have also been performed [27]. Moreover, niobium containing glasses have several interesting non-linear properties, which make them attractive materials for ultra-fast switching devices [28, 29]. Further, second harmonic generation (SHG) was observed in borophosphate glasses containing Nb_2O_5 after a thermal poling treatment [30]. The addition of glass modifiers such as Nb_2O_5 in phosphate glasses breaks the P–O–P linkages and generates non-bridging oxygens as well as electric dipoles. The latter can contribute to an increase of the linear refractive index; the amount of increase depends upon Nb_2O_5 concentration [31].

The addition of PbO is expected to make these glasses more moisture resistant, since PbO, in contrast to the conventional alkali/alkaline earth oxide/halide modifiers, has the ability to form stable glasses due to its dual role: one as modifier (with PbO_6 structural units, if Pb–O is ionic) and the other as glass former (with PbO_4 structural units, if Pb–O is covalent). The covalent character of PbO is probably due to the strong interaction of easily polarizable valence shells of Pb^{2+} ions with the highly polarizable O^{2-} ion [32]. Such glasses may also be of particular interest for non-linear optical effects, as shown for the RE^{3+}-doped PbO complex glasses. The infrared (IR) harmonic and anharmonic electron–phonon modes are expected to contribute significantly to the non-linear optical susceptibilities in these glasses [33]. In view of the above merits of phosphate glasses, Nb_2O_5 and PbO, which act as glass modifier and glass modifier/former, respectively, it is interesting to study the optical properties of Sm^{3+} ions in P_2O_5–PbO–Nb_2O_5 glass with varying pressure.

The concentration dependence of luminescence properties of Sm^{3+} ions in the P_2O_5–PbO–Nb_2O_5 glass has been studied in our earlier paper [34], where we reported Judd–Ofelt analysis, radiative properties such as radiative transition probabilities, lifetime of excited states, branching ratios, emission cross-section, non-radiative rate, etc. The present study describes the pressure dependent luminescence properties of Sm^{3+} ions in the same host.

2. Experimental techniques

The glass sample of molar composition $55P_2O_5 + 39.5PbO + 5Nb_2O_5 + 0.5Sm_2O_3$ (PPNSm05) was prepared by the melt quenching method [34]. The emission spectra were recorded with a double monochromator equipped with a photomultiplier tube. The 476.5 nm line of an Ar^+ laser was used as the excitation source. The resolution of the monochromator depends on the slit width (typically set at 2.0 cm^{-1}) and wavelength.

A special gasketed diamond anvil cell (DAC) was used to generate hydrostatic pressures up to 23.6 GPa at room temperature. A piece of PPNSm05 glass was placed together with a ruby pressure sensor into an 80 μm diameter hole of a stainless steel (Inconel X 750) gasket of 200 μm thickness. A mixture of methanol:ethanol:water (16:3:1) was used as the pressure transmitting medium. The gasket containing the sample and pressure transmitting fluid was then compressed by the two opposed anvils of the DAC. The pressure and the hydrostatic conditions experienced by the sample were determined by the shift and broadening of the ruby R_1 lines [35]. A mechanical chopper in connection with a multi-channel scalar allowed for lifetime measurements in the range from 2 μs to 2 s.

3. Decay curve analysis

Fluorescence decay curves of the $^4G_{5/2}$ level of Sm^{3+} ions, following pulsed excitation in the PPNSm05 glass, exhibit a non-exponential nature at all pressures and can be well described by the equation [36]

$$I(t) = A_1 \exp\left(-\frac{t}{\tau_1}\right) + A_2 \exp\left(-\frac{t}{\tau_2}\right) \tag{1}$$

and the average lifetime (τ_{avg}) can be estimated as

$$\tau_{avg} = \frac{A_1\tau_1^2 + A_2\tau_2^2}{A_1\tau_1 + A_2\tau_2}. \tag{2}$$

The excited donor ions can relax by direct energy transfer to acceptor ions or after migration of the excitation among donor ions until an acceptor is reached. If the donor and acceptor ions are randomly distributed in the host and the migration processes are negligible compared to donor–acceptor energy transfer, then the temporal evolution of the donor population, following pulsed excitation, is given by the well known Inokuti–Hirayama (IH) model equation [37],

$$I(t) = I(0)\exp\left\{-\frac{t}{\tau_0} - Qt^{3/S}\right\} \tag{3}$$

Table 1. Values for the Padè approximate coefficients in equation (5) for different multipolar interactions.

S	a_1	a_2	b_1
6	10.866	15.500	8.743
8	17.072	35.860	13.882
10	24.524	67.909	20.290

where Q is the energy transfer parameter and is given by

$$Q = \frac{4\pi}{3} N_0 \Gamma\left(1 - \frac{3}{S}\right)(C_{DA})^{3/S} \tag{4}$$

where N_0 is the concentration of acceptors, which is almost identical with the total concentration of RE ions, and $\Gamma(x)$ is the gamma function. The latter is equal to 1.77 for dipole–dipole ($S = 6$), 1.43 for dipole–quadrupole ($S = 8$) and 1.3 for quadrupole–quadrupole ($S = 10$) interactions, respectively. However, if migration processes among donors are important then the problem is more complex and different approximations have been developed in order to analyze this situation. One possibility is to consider the energy migration as a diffusion process [38–41]. This method was adopted by Yokota and Tanimoto (YT) [39], who obtained a simple expression for the temporal evolution of excited donors. The validity of this expression is limited to strong donor–acceptor interaction with weak diffusion. From the fit of this expression to experimental decay curves, the diffusion parameter among donors and the energy transfer parameter from donors to acceptors can be calculated. Unfortunately, this model is restricted to energy transfer processes with dipole–dipole interaction ($S = 6$) among donors and acceptors. Martin *et al* [42] obtained a generalization of the YT expression for emission intensity as a function of time for any kind of multipolar interaction, i.e.

$$I(t) = I(0) \times \exp\left\{-\frac{t}{\tau_0} - Qt^{3/S}\left(\frac{1 + a_1X + a_2X^2}{1 + b_1X}\right)^{(S-3)/(S-2)}\right\} \tag{5}$$

where

$$X = DC_{DA}^{-2/S} t^{1-2/S} \tag{6}$$

and D is the diffusion coefficient ($cm^2\ s^{-1}$) that characterizes the energy transfer processes between donors, C_{DA} is the donor–acceptor coupling constant, $C_{DA} = \frac{R_0^S}{\tau_0}$, where R_0 is the critical transfer distance (Å), τ_0 is the radiative lifetime (μs) and a_1, a_2 and b_1 are Padé approximate coefficients, which depend on the type of multipolar interaction, and are presented in table 1. From equation (5), assuming a dipole–dipole interaction ($S = 6$) the YT expression is reproduced, whereas the IH expression is obtained when the migration between donors is negligible ($D = 0$).

In the models given by equations (3) and (5), energy transfer due to cross-relaxation processes between RE ions is well described, regardless of whether these processes are assisted by phonons or not. Usually, in energy transfer processes assisted by phonons the values of the C_{DA} parameter and hence the transfer probability and the Q parameter are much lower than those in the resonant situation. Moreover, if the distance between optically active ions decreases (due to an increase in the pressure or doping concentration) then one may expect an increase in the Q parameter and, as a consequence, faster fluorescence decays.

On the other hand, in the generalized YT model given by equation (5) the energy transfer processes among the donors, characterized by the parameter D, are also taken into account. If these processes are efficient, the energy could migrate among the donors until a nearby acceptor is reached and may result in an increase in the transfer efficiency. Even in samples with only one type of RE ion, playing the roles of donor and acceptor, the cross-relaxation and the migration processes could compete.

For continuous excitation, the emission intensity is proportional to the concentration of excited ions N^*, which can be expressed as a function of the relative donor quantum yield of luminescence, η/η_0 [43], i.e.

$$N^* \propto \tau_0 \frac{\eta}{\eta_0} \tag{7}$$

where the relative donor quantum yield of luminescence is defined by [44]

$$\frac{\eta}{\eta_0} = \frac{1}{\tau_0}\int_0^\infty I_{exp}(t)\,dt \tag{8}$$

η and η_0 represent the relative donor quantum yield with and without acceptors, respectively. Thus $\frac{\eta}{\eta_0}$ becomes unity when energy transfer to acceptors is negligible.

4. Results and discussion

4.1. Study of pressure dependence of multiplet energy positions and crystal-field splittings

The luminescence spectra of Sm^{3+} ions in PPNSm05 glass obtained in the spectral domain of 15 300–18 000 cm^{-1} at different (increasing or decreasing) pressures are shown in figure 1. The spectral shapes are similar to those obtained in K–Ba–Al-phosphate (phosphate) [45], lithium borate (L5BS) [46], lithium fluoroborate (L5FBS) [46] and tellurite (TKNSm10) [47] glasses. The spectral peaks are assigned to the $^4G_{5/2} \rightarrow {}^6H_{9/2}$, $^6H_{7/2}$ and $^6H_{5/2}$ transitions, which correspond to the spectral regions 15 300–15 700 cm^{-1}, 16 000–17 100 cm^{-1} and 17 300–17 900 cm^{-1}, respectively. The peak positions are presented in table 2. It can be observed from figure 1 that peak positions are shifted towards the lower energy region, indicating a continuous red shift under increasing pressure, and are plotted in figure 2. The $^4G_{5/2} \rightarrow {}^6H_{5/2}$ and $^4G_{5/2} \rightarrow {}^6H_{7/2}$ multiplets show partially lifted degeneracy, since the emission peaks are split into two Stark components that are well resolved even at high pressure. The magnitude of splitting increases for the $^4G_{5/2} \rightarrow {}^6H_{5/2}$ and $^4G_{5/2} \rightarrow {}^6H_{7/2}$ transitions from 129 and 133 cm^{-1} at ambient pressure to 211 and 259 cm^{-1} at 23.6 GPa, respectively. The variation of the CF splittings with pressure is shown in figure 3. This implies that pressure gradually increases the CF strength and simultaneously the splitting due to a continuous decrease of the average distance between the Sm^{3+} ion and ligands (oxygen ions) [10].

Table 2. Emission peak positions for the $^4G_{5/2} \rightarrow {}^6H_J$ ($J = 9/2, 7/2$ and $5/2$) transitions, crystal-field splitting (CFS) for $^4G_{5/2} \rightarrow {}^6H_{5/2}$ and $^4G_{5/2} \rightarrow {}^6H_{7/2}$ transitions, fluorescence lifetimes (τ_{avg}, μs) of the $^4G_{5/2}$ level, energy transfer parameter (Q), donor–acceptor interaction parameter (C_{DA}, $\times 10^{-40}$ cm^6 s^{-1}), diffusion parameter (D, $\times 10^{-13}$ cm^2 s^{-1}) and relative donor quantum yield (η/η_0) for Sm^{3+} ions in PPNSm05 glass at different pressures (GPa).

	Peak positions (cm^{-1})			CFS (cm^{-1})						
Pressure	$^6H_{9/2}$	$^6H_{7/2}$	$^6H_{5/2}$	$^6H_{5/2}$	$^6H_{7/2}$	τ_{avg}	Q	C_{DA}	D	η/η_0
(a) Pressure increasing										
0	15 536	16 764	17 837	129	133	2294	0.12	0.18	0.14	0.84
3.9	15 503	16 725	17 803	155	203	2079	0.12	0.19	0.36	0.77
6.8	15 499	16 712	17 793	194	247	1867	0.13	0.21	0.60	0.70
8.9	15 484	16 694	17 770	208	251	1782	0.13	0.23	0.75	0.66
10.3	15 498	16 709	17 783	208	249	1607	0.19	0.46	0.89	0.58
13.2	15 482	16 695	17 766	207	246	1406	0.22	0.63	1.25	0.50
16.4	15 456	16 673	17 742	207	248	1380	0.27	0.98	1.28	0.47
21.3	15 449	16 652	17 719	209	251	850	0.35	1.63	2.76	0.31
23.6	15 437	16 646	17 709	211	259	643	0.40	2.12	4.17	0.24
(b) Pressure decreasing										
15.5	15 474	16 689	17 758	200	230	1248	0.27	1.00	1.57	0.44
8.8	15 505	16 722	17 779	181	220	1701	0.22	0.65	0.01	0.62
1.0	15 518	16 738	17 816	150	160	2221	0.10	0.15	0.00	0.81

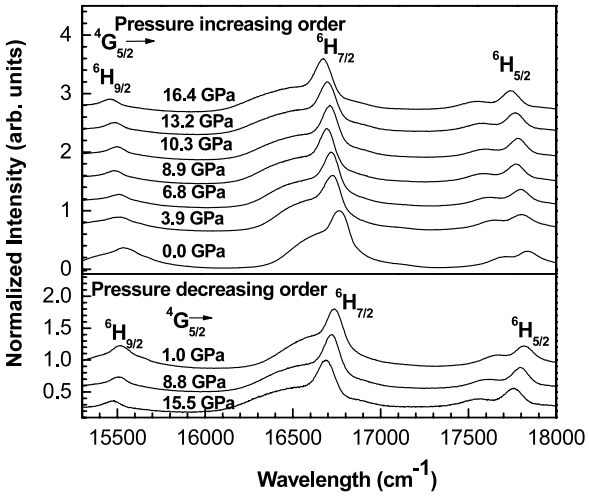

Figure 1. Normalized emission spectra of Sm^{3+}-doped PPNSm05 glass with pressure.

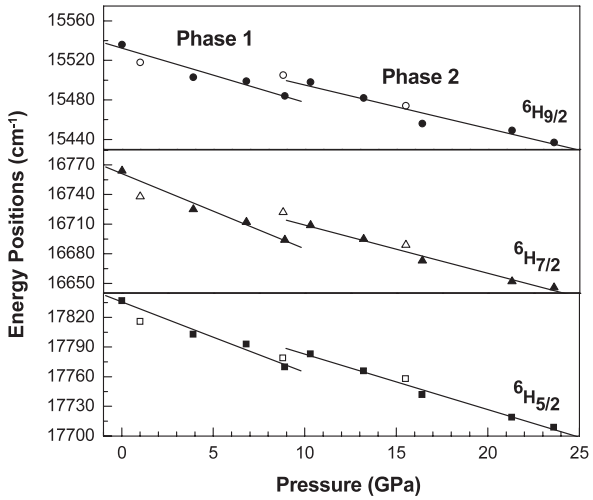

Figure 2. Variation of peak positions for the emission $^4G_{5/2} \rightarrow {}^6H_J$ ($J = 5/2, 7/2$ and $9/2$) bands of Sm^{3+}-doped PPNSm05 glass with pressure. The solid (open) symbols represent increasing (decreasing) pressure. The solid line is a linear fit to the experimental data for increasing pressure in both phases.

A closer inspection of figures 1 and 2, however, indicates that beside the general shift of the emission peaks towards lower energy there is a discontinuity in the shifts up to 8.9 GPa (referred to as phase 1) and from 10.3 to 23.6 GPa (referred to as phase 2). A similar discontinuity is obvious in the crystal-field splittings of the $^4G_{5/2} \rightarrow {}^6H_{5/2}$ and $^6H_{7/2}$ levels shown in figure 3. Therefore, the observed discontinuity in all multiplet positions between 9 and 10 GPa suggests that a phase transition has occurred in the glass matrix, which will be investigated in detail in future work. It should be mentioned that a pressure-induced phase transition was also observed in an optical study of Eu^{3+}:YVO_4 [48, 49].

The shift of the peak positions in both phases as a function of pressure can be described by a linear equation,

$$E_i(p) = E_i(0) + \alpha_i p \qquad (9)$$

where $E_i(p)$ are the energies (in cm^{-1}) of the studied transitions ($^4G_{5/2} \rightarrow {}^6H_{9/2}$, $^6H_{7/2}$ and $^6H_{5/2}$) at pressure p (in GPa) and α_i indicates the slope of the straight line which gives the energy shift per GPa. The α_i values for increasing pressures are presented in table 3. The negative sign of α_i indicates the red shift that results from various interaction mechanisms. For instance, the shift of the LS manifolds with respect to each other is due to variations in electrostatic interactions. For a given LS value, the shift of each splitting for a J manifold results from the variation of the spin–orbit coupling parameter (ξ_{4f}) [50]. For a given LSJ value, the shift of the Stark levels with respect to each other arises from the variations in strength and symmetry of the CF around the Sm^{3+} ions.

Table 3. The fitting parameter α_i (equation (9)) obtained for the peak positions of the $^4G_{5/2} \rightarrow {}^6H_J$ ($J = 5/2, 7/2$ and $9/2$) transitions of Sm^{3+} ions in the present PPNSm05 glass in two different phases and reported L5BS, K–Ba–Al-phosphate and TKNSm10 glasses with increasing pressure.

	Energy shift (α_i, cm^{-1} GPa^{-1})				
	PPNSm05				
Term	Phase 1	Phase 2	L5BS [46]	K–Ba–Al-phosphate [45]	TKNSm10 [47]
$^6H_{5/2}$	−7.1	−5.6	−4.2	−2.7	−3.9
$^6H_{7/2}$	−7.6	−4.9	−4.2	−2.6	−3.3
$^6H_{9/2}$	−5.5	−4.4	−4.4	−2.4	−3.1

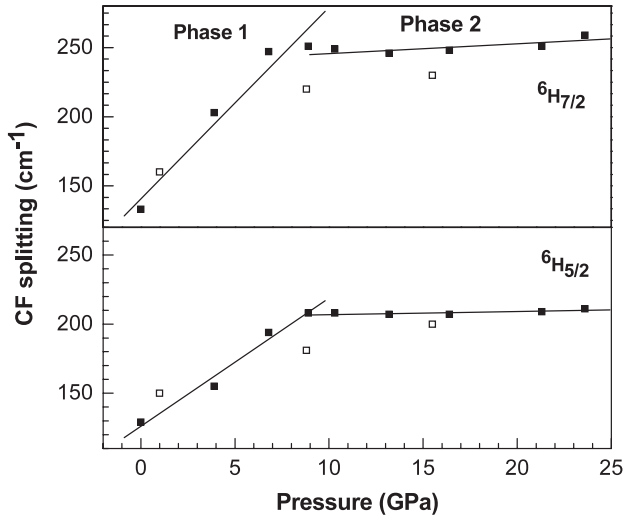

Figure 3. Crystal-field splitting of the $^4G_{5/2} \rightarrow {}^6H_{5/2}$ and $^6H_{7/2}$ levels of Sm^{3+}-doped PPNSm05 glass with pressure. The solid (open) symbols represent increasing (decreasing) pressure. The solid line is a linear fit to the experimental data for increasing pressure in two different phases.

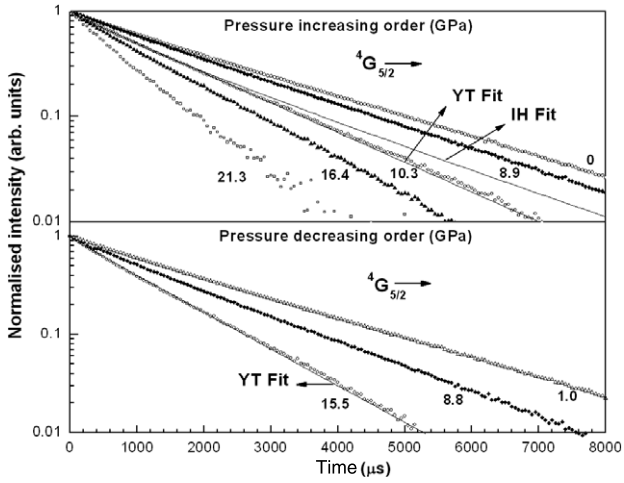

Figure 4. Decay profiles for the $^4G_{5/2}$ level in Sm^{3+}-doped PPNSm05 glass with pressure. The IH and YT model fits for $S = 6$ for decay curve at 10.3 GPa (increasing pressure) and the YT fit for the decay curve at 15.5 GPa (decreasing pressure) are shown.

Thus, the measured shifts of each luminescence peak as well as their splitting with pressure can provide the data necessary for probing the electrostatic, spin–orbit and CF interactions. As can be seen from figure 2 and table 3, the pressure coefficients α_i of the red shift are larger in phase 1 than in phase 2. Table 3 also demonstrate that the pressure coefficients α_i in both phases of the present PPNSm05 glass are larger than those in Sm^{3+}-doped phosphate [45], L5BS [46] and TKNSm10 [47] glasses.

As can be seen from figure 3, the crystal-field splitting (CFS) increases sharply up to 8.9 GPa (phase 1), while above 8.9 GPa the increase is only marginal (phase 2). A quantitative estimation of the CF strength for Sm^{3+}-doped systems has not been made due to the complex electronic structure of Sm^{3+} ions [51]. In Sm^{3+}:phosphate [45] glass the magnitude of CFS for $^4G_{5/2} \rightarrow {}^6H_{5/2}$ transition increases from 128 to 225 cm^{-1} as pressure is raised from 0 to 24.4 GPa, whereas in L5BS [46] glass it increases from 171 to 266 cm^{-1} when pressure is increased from ambient to 27.2 GPa, and in TKNSm10 [47] glass the CFS increases from 158 to 214 cm^{-1} when the pressure is increased from 0 to 14.6 GPa. These increases in CFS values can be attributed to a greater reduction of the Slater parameter (F^k) and the spin–orbit coupling parameter (ξ) in the present PPNSm05 glass than in phosphate, L5BS and TKNSm10 glasses due to changes in the overlap of the ligand orbitals with the 4f wavefunctions of Sm^{3+} ions with increasing pressure.

To summarize this section, a strong red shift and a broadening of the fluorescence lines have been observed for the $^4G_{5/2} \rightarrow {}^6H_{5/2,7/2,9/2}$ transition of Sm^{3+} ions in PPNSm05 glass up to 8.9 GPa. The former effect is due to an increase in the covalency in the Sm^{3+}–ligand bonds as they are shortened by compression, whereas the latter effect is due to the variation of the local fields, which is accompanied by the formation of strong CF environments for the Sm^{3+} ions as a consequence of the increasing distortion of the glass network with the pressure, that modulate the bond angles and lengths [52]. A detailed analysis of the properties of phase 2 of PPNSm05 glass must wait for further investigations, e.g. a study of the phase transition as a function of Nb content.

4.2. Study of pressure-induced changes in lifetime and derived parameters

The fluorescence decay curves of the $^4G_{5/2}$ level in the PPNSm05 glass have been measured as a function of pressure up to 23.6 GPa and are shown in figure 4 for increasing and decreasing pressures. The decay profile exhibits non-exponential nature in the entire pressure range studied accompanied by a fast decrease of lifetimes. This behavior is attributed to (1) the energy transfer between the Sm^{3+} ions in different sites, (2) energy transfer between the Sm^{3+} ions

and impurities such as transition metal ions and/or (3) energy transfer between Sm^{3+} ions and pressure-induced enhanced defect centers. The non-exponential decay curves have been fitted to both the IH model (equation (3)) and the generalized YT model (equation (5)) for $S = 6$, 8 and 10, in order to probe the mechanisms of the energy transfer involved. Both IH and YT model fits for the decay curve at 10.3 GPa (increasing pressure) and a YT model fit for the decay curve at 15.5 GPa (decreasing pressure) are shown in figure 4. As can be seen from figure 4, the decay curves are much better fitted by the YT model than by the IH model, which indicates that the energy migration also plays an important role in the present glass. The decay curves are well fitted to $S = 6$, indicating that the energy transfer process is of dipole–dipole type. Similar results have been obtained by Jayasankar *et al* [45, 46], Reisfeld *et al* [53] and Zhang *et al* [54]. On the other hand, Lavin *et al* [10] obtained best fits for quadrupole–quadrupole interactions under high pressure for borate and fluoroborate glasses. Mahato *et al* [55] for oxyfluoroborate glasses and Chang and Powell [56] for $CaWO_4$ crystals obtained best fits for quadrupole–quadrupole interactions at ambient conditions.

The energy migration enhances the cross-relaxation probability as it spreads the excitation energy into the host material. In this sense, these energy transfer probabilities and efficiencies are features directly related to the pump efficiency. The energy transfer process occurs between RE ions mediated mainly by multipolar interactions. It is a common practice to attribute the dipole–dipole type interaction to treat the energy transfer among impurities diluted in a solid medium. However, higher-order energy transfer mechanisms, such as dipole–quadrupole or quadrupole–quadrupole, may be important in RE doped samples if the electronic transitions involved in the energy transfer process are electric quadrupole permitted and the interagent ions are close enough [57, 58].

The experimental decay curves are fitted to equation (5) for $S = 6$ by taking lifetime (τ_0) at lower concentration (0.1 mol%) [34] where the decay curves exhibit exponential nature. The energy transfer (Q), donor–acceptor interaction (C_{DA}), and diffusion (D) parameters have been calculated as functions of pressure and are presented in table 2. The values of Q parameter for all the pressures are found to be higher than 0.11, that of 2.0 mol% Sm^{3+}-doped PPNSm20 glass at ambient conditions [34]. Similarly, the C_{DA} values above 10.3 GPa are larger than 0.29, observed for 2.0 mol% Sm^{3+}-doped PPNSm20 glass at ambient conditions [34]. The D values found in this glass are in the same range as those found in Tm^{3+}, Ho^{3+} and Tm^{3+}–Ho^{3+} co-doped alkali niobium tellurite glasses sensitized by Yb^{3+} [59]. The variation of Q with pressure follows the opposite trend to that of the lifetime (figure 5), indicating an increase of energy transfer processes with pressure, which is also reflected in the increase of non-exponential nature in the decay curves and decrease of lifetimes.

Average lifetimes (τ_{avg}) of the $^4G_{5/2}$ level for all the studied pressures have been determined from the non-exponential decay curves using equation (2) and are collected in table 2. It is interesting to note that the τ_{avg}, Q, C_{DA} and D values are found to be varying continuously and therefore

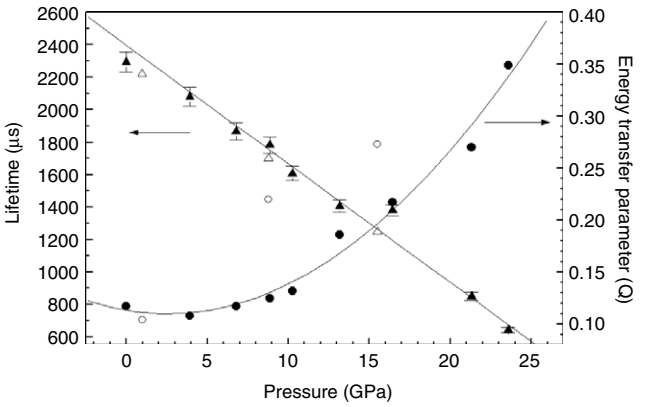

Figure 5. Variation of lifetime for the $^4G_{5/2}$ level and energy transfer parameter (Q) in the Sm^{3+}-doped PPNSm05 glass with pressure. The solid (open) symbols represent increasing (decreasing) pressure. The solid lines are guides to the eye.

less influenced by the phase transitions. It is worth noting that the lifetime at 6.8 GPa (1.87 ms) is similar to that (1.90 ms) obtained for the 1.0 mol% Sm^{3+}-doped PPNSm glass at ambient conditions [34]. Similarly, the lifetimes at 16.4 GPa (1.38 ms) and 21.3 GPa (0.85 ms) are close to those obtained for 2.0 mol% (1.38 ms) and 4.0 mol% (0.83 ms), respectively, at ambient conditions for Sm^{3+}:PPNSm glasses [34]. This means that a pressure of around 6.8, 16.4 and 21.3 GPa corresponds to a two, four and eightfold increase in the effective concentration of Sm^{3+} ions, respectively, which is due to the reduced volume with increase in pressure.

Variation of lifetime of the $^4G_{5/2}$ level with pressure is presented in figure 5. As can be seen from table 2 and figure 5, the lifetimes of the $^4G_{5/2}$ level continuously decreases with increase in pressure. This decrease in lifetimes with increase in pressure could be explained either by an increase in the multiphonon de-excitation probabilities or by an increase in the electronic transition probabilities. But in the case of Sm^{3+} ions, one can expect pure radiative decay from the $^4G_{5/2}$ level due to the large energy gap of about 7000 cm^{-1} to its lower $^6F_{11/2}$ level, preventing an appreciable multiphonon relaxation probability. The latter effect could be explained by stronger crystal fields as a result of changes in the Sm^{3+} ion local structure under pressure. The increase in pressure, which can change the bond angles and lengths, causes a gradual increase in the CF strengths around the Sm^{3+} ions, which is also reflected by the increase in the CF splittings of the $^4G_{5/2} \rightarrow {}^6H_{5/2}$ and $^4G_{5/2} \rightarrow {}^6H_{7/2}$ transitions with pressure (figure 3). As a consequence, a stronger mixing of opposite parity configurations with the $4f^5$ configuration due to the odd CF Hamiltonian and an increase in the transition probabilities may occur. The pressure-induced volume reduction causes stronger crystal fields and therewith enhanced configuration interactions, which increase the electronic transition probabilities and decrease the lifetimes of the fluorescent levels in the Sm^{3+}-doped PPNSm05 glass. A similar explanation has been used to explain the decrease in lifetimes with pressure in Sm^{3+}:lithium fluoroborate glass [10, 46].

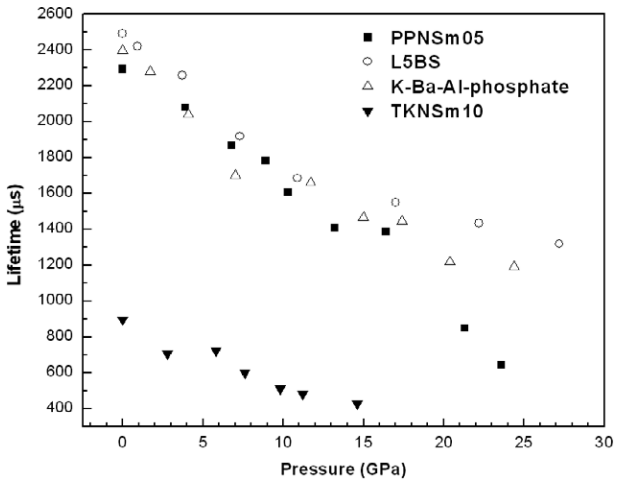

Figure 6. Variation of lifetime for the $^4G_{5/2}$ level of Sm^{3+} ions in PPNSm05, L5BS [46], K–Ba–Al-phosphate [45] and TKNSm10 [47] glasses as a function of pressure.

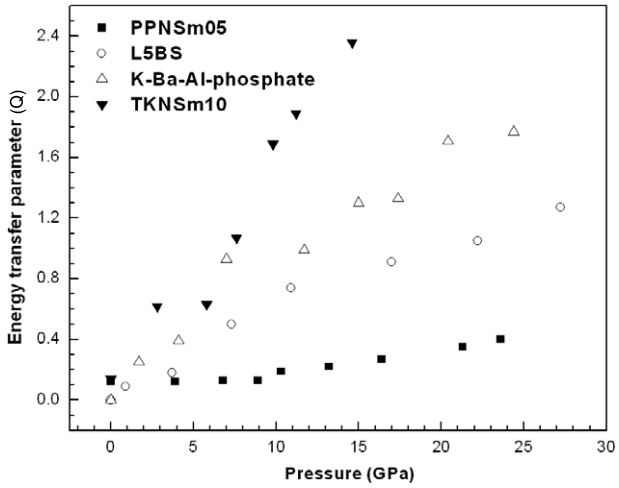

Figure 7. Variation of energy transfer parameter in Sm^{3+}-doped PPNSm05, L5BS [46], K–Ba–Al-phosphate [45] and TKNSm10 [47] glasses as a function of pressure.

Figure 6 compares the variation of lifetime for the $^4G_{5/2}$ level of Sm^{3+} ions with increasing pressure in different hosts. As can be seen from the figure, the lifetimes are lowest in TKNSm10 glass due to the higher covalency of the Sm–O bond. The lifetimes in L5BS, phosphate and the present PPNSm05 glasses are more or less similar. The BaO-based phosphate glass has a slightly longer lifetime (2397 μs) than the PbO-based phosphate glass (2294 μs) at ambient pressure. This could be due to the more ionic nature (strength) of Ba–O bonds than Pb–O bonds. From figure 6, it can also be seen that the quenching of lifetimes with increasing pressure in the present PPNSm05 glass is larger compared to L5BS, phosphate and TKNSm10 glasses due to the presence of the Pb/Nb content in the PPNSm05 glass.

The energy transfer parameters (Q) in different glass hosts are compared in figure 7, which clearly indicates that the energy transfer parameter is largest in the TKNSm10 glass and smallest in the PPNSm05 glass. The magnitude of Q values follows the order of PPNSm05 < L5BS < phosphate < TKNSm10 glasses. This indicates higher migration energy among the donors rather than an energy transfer by cross-relaxation between Sm^{3+} ions in the PPNSm05 glass.

According to equation (7), the luminescence intensity is proportional to the concentration of the excited ions (N^*) which depends on the lifetime τ and relative donor quantum yield η/η_0 of the luminescence. The latter values, obtained from equation (8) at different pressures, are shown in table 2 and in figure 8. From table 2 and figures 5 and 8, it is evident that both the lifetime τ and relative donor quantum yield η/η_0 decrease by about a factor of 3.5 from ambient conditions to 23.6 GPa for the PPNSm05 glass. But Jayasankar *et al* [46] observed only a twofold decrease of lifetime as well as relative quantum yield from ambient to ~26.0 GPa for both L5BS and L5FBS glasses. This difference could be due to the different chemical composition and resulting changes in the local structure around Sm^{3+} ions in the PPNSm05 glass.

The few results obtained with decreasing pressure are shown in figures 1–5 and 8 as well as in table 2. As in previous studies, the data points are less accurate than those with increasing pressure, but follow the general trend. As can be seen from figure 2, these few data may indicate that the phase transition takes place at lower pressure when releasing the pressure. As already mentioned, future studies must be devoted to this phase transition.

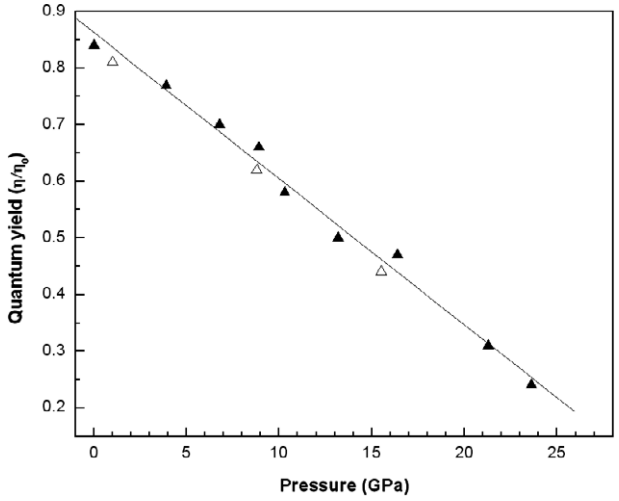

Figure 8. Variation of the relative donor quantum yield of luminescence for the $^4G_{5/2}$ level of the Sm^{3+} ions in the PPNSm05 glass as a function of pressure. The solid (open) symbols represent the increasing (decreasing) pressure.

5. Conclusions

The luminescence properties of Sm^{3+} ions in PPNSm05 glass have been investigated under pressure up to 23.6 GPa. A discontinuity from the linear trends in energy level shifts and crystal-field splittings indicates that a pressure-induced phase transition has occurred around 9–10 GPa in the present glass system. Overall, a continuous red shift in peak positions of emission spectra has been observed in both phases with increasing pressure, which is attributed to an expansion of the 4f wavefunctions with increasing covalency. The

enhancement of crystal-field splitting of $^4G_{5/2} \rightarrow {}^6H_{7/2}$ and $^4G_{5/2} \rightarrow {}^6H_{5/2}$ transitions with increasing pressure is due to the decrease in volume and in turn a simultaneous decrease of the average distance between Sm^{3+} ions and ligand ions. The decay profiles exhibit non-exponential nature for all pressures accompanied by shortening of lifetimes. The non-exponential decay curves are well fitted to the generalized Yokota–Tanimoto model for $S = 6$, indicating that the mechanism of interaction for energy transfer between donor and acceptor is of dipole–dipole type. The energy transfer, donor–acceptor interaction and diffusion parameters increase with increasing pressure due to energy migration followed by energy transfer due to cross-relaxation between Sm^{3+} ions. The relative donor quantum yield decreases with increasing pressure. The lifetime for the $^4G_{5/2}$ level is found to decrease with increasing pressure, which could be due to an increase in the electronic transition probabilities, resulting from the increased crystal-field strength around Sm^{3+} ions.

Acknowledgments

This work has been supported through a Major Research Project funded by the University Grants Commission (F.32-28/2006(SR) dt. 19-03-2007), Government of India. One of the authors (CKJ) is grateful to Department of Physik, Universität Paderborn, Germany, for his stay as a guest scientist.

References

[1] Hayakawa T and Nogami M 2001 *J. Appl. Phys.* **90** 2200
[2] Dantas N O and Qu F 2003 *Physica* B **327** 79
[3] Digonnet M J (ed) 1993 *Rare Earth Doped Fiber Lasers and Amplifiers* (New York: Dekker)
[4] Jerez V A, De Araujo C B and Messaddeq Y 2004 *J. Appl. Phys.* **96** 2530
[5] Peng B, Qiu X M, Jiang L, Fan Z C and Huang W 2004 *Appl. Phys. Lett.* **85** 1910
[6] Dai S X, Zhang J J, Li S G, Yang G H, Xu S Q, Wang G N and Hu L L 2004 *J. Mater. Sci. Technol.* **20** 668
[7] Bray K L 2001 *Topics in Current Chemistry* vol 213 (Berlin: Springer)
[8] Nogami M and Suzuki K 2002 *Adv. Mater.* **14** 923
[9] Qiu J, Miura K, Suzuki T and Mitsuyu T 1999 *Appl. Phys. Lett.* **74** 10
[10] Lavin V, Martin I R, Jayasankar C K and Tröster Th 2002 *Phys. Rev.* B **66** 064207
[11] Görller-Walrand C and Binnemans K 1998 *Handbook on the Physics and Chemistry of Rare Earths* vol 25, ed K A Gschneidner Jr and L Eyring (New York: Elsevier) chapter 167
[12] Jayasankar C K and Babu P 2000 *J. Alloys Compounds* **307** 82
[13] Lacha L M, Balda R, Fernandez J and Adam J L 2004 *Opt. Mater.* **25** 193
[14] Abd El-Ati M I and Higazy A A 2000 *J. Mater. Sci.* **35** 6175
[15] Suratwala T I, Steele R A, Wike G D, Campbell J H and Takenchi K 2000 *J. Non-Cryst. Solids* **263/264** 213
[16] Sales B C and Boatner L A 1988 Lead–iron phosphate glass *Radioactive Waste Forms for the Future* ed W Lutze and R C Ewing (Amsterdam: North-Holland) p 193
[17] Khafagy A H, ElpRabaie S M, Higazy A A and Eid A S 2000 *Indian J. Phys.* A **74** 433
[18] Donald I W 1993 *J. Mater. Sci.* **28** 2841
[19] Pyare R, Lal L J, Joshi V C and Singh V K 1996 *J. Am. Ceram. Soc.* **79** 1334
[20] Nikorov N V, Kolobkova E V and Zakhvatova M B 1993 *Sov. J. Glass Phys. Chem.* **19** 66
[21] Sombra A S B 1990 *Opt. Quantum Electron.* **22** 335
[22] Payne S A, Marshall C D, Bayramian A, Wike G D and Hayden J S 1995 *Appl. Phys.* B **61** 157
[23] Balda R, Fernandez J, Arriandiaga M A, Voda M and Fernandez-Navarro J M 2004 *Opt. Mater.* **25** 157
[24] Fernandez J, Iparraguire I, Balda R, Azkargorta J, Voda M and Fernandez-Navarro J M 2004 *Opt. Mater.* **25** 185
[25] Chen D D, Liu Y H, Zhang Q Y, Deng Z D and Jiang Z H 2005 *Mater. Chem. Phys.* **90** 78
[26] Flambard A, Montagne L, Delevoye L, Palavit G, Amoureux J-P and Vieau J-J 2004 *J. Non-Cryst. Solids* **345** 75
[27] Martinelli J R, Sene F F and Gomes L 2000 *J. Non-Cryst. Solids* **263** 263
[28] Cardinal T, Fargin E, Le Flem G, Couzi M, Canioni L, Segonds P, Sarger L, Ducasse A and Adamietz D 1996 *Eur. J. Solid State Inorg. Chem.* **33** 597
[29] Ebendorff-Heidepriem H, Ehrt D, Bettinelli M and Speghini A 1999 Rare-earth-doped materials and devices III *Proc. SPIE* **3622** 19–30
[30] Nazabal V, Fargin E, Videau J J, Le Flem G, Le Calvez A, Montant S, Freusz E, Ducasse A and Couzi M 1997 *J. Solid State Chem.* **133** 529
[31] Sene F F, Martinelli J R and Gomes L 2004 *J. Non-Cryst. Solids* **348** 63
[32] Srinivasa Rao G and Veeraiah N 2002 *J. Phys. Chem. Solids* **63** 705
Raghavaiah B V, Laxmikanth C and Veeraiah N 2004 *Opt. Commun.* **35** 341
[33] Wasylak J, Kityk I V and Kucharski J 2003 *Phys. Status Solidi* a **199** 515
[34] Praveena R, Venkatramu V, Babu P and Jayasankar C K 2008 *Physica* B **403** 3527
[35] Holzapfel W B 2003 *J. Appl. Phys.* **93** 1813
[36] Fuji T, Kodaira K, Kawauchi O, Tanaka N, Yamashita H and Anpo M 1997 *J. Phys. Chem.* B **101** 10631
[37] Inokuti M and Hirayama F 1965 *J. Chem. Phys.* **43** 1978
[38] Triflaj M 1958 *Czech. J. Phys.* **8** 510
[39] Yokota M and Tanimoto O 1967 *J. Phys. Soc. Japan* **22** 779
[40] Chow H C and Powell R C 1980 *Phys. Rev.* B **21** 3785
[41] Parent C, Lurin C, Le Flem G and Hagenmuller P 1986 *J. Lumin.* **36** 49
[42] Martin I R, Rodriguez V D, Rodriguez-Mendoza U R, Lavin V, Montoya E and Jaque D 1999 *J. Chem. Phys.* **111** 1191
[43] Eisenthal K B and Siegel S 1964 *J. Chem. Phys.* **41** 652
[44] Eisenthal K B *et al* 1984 *Energy Transfer Processes in Condensed Matter* (*NATO Advanced Study Institute Series B: Physics* vol 114) ed B Di Bartolo (New York: Plenum)
[45] Jayasankar C K, Balakrishnaiah R, Babu P, Tröster Th, Sievers W and Wortmann G 2006 *High Press. Res.* **26** 349
[46] Jayasankar C K, Venkatramu V, Babu P, Tröster Th, Sievers W, Wortmann G and Holzapfel W B 2005 *J. Appl. Phys.* **97** 093523
[47] Jayasankar C K, Upendra Kumar K, Venkatramu V, Babu P, Tröster Th, Sievers W and Wortmann G 2008 *J. Lumin.* **128** 718
[48] Chen G, Stump N A, Haire R G, Peterson J R and Abraham M M 1992 *J. Phys. Chem. Solids* **53** 1253
[49] Chen G, Stump N A, Haire R G, Peterson J R and Abraham M M 1992 *Solid State Commun.* **84** 313
[50] Chen G, Stump N A, Haire R G, Burns J B and Peterson J R 1994 *High Press. Res.* **12** 83

[51] Renuka Devi A, Jayasankar C K and Reid M F 1994 *Phys. Rev.* B **49** 12551
[52] Soga N, Hirao K, Yoshimoto M and Yamamoto H 1988 *J. Appl. Phys.* **63** 4451
[53] Reisfeld R, Bornstein A and Boehm L 1975 *J. Solid State Chem.* **14** 14
[54] Zhang Z, Jiang X, Li Z, Wu P and Xu S 1988 *J. Lumin.* **40** 657
[55] Mahato K K, Rai D K and Rai S B 1998 *Solid State Commun.* **108** 671
[56] Chang H and Powell R C 1975 *Phys. Rev. Lett.* **35** 734
[57] Gomes L, Courrol L C, Tarelho L V G and Ranieri I M 1996 *Phys. Rev.* B **54** 3825
[58] Basiev T T, Orlovskii Yu V and Privis Yu S 1996 *J. Lumin.* **69** 187
[59] Courrol L C, Tarelho L V G, Gomes L, Vieira N D Jr, Cassanjes F C, Messaddeq Y and Ribeiro S J L 2001 *J. Non-Cryst. Solids* **284** 217